arXiv:1612.08748v1 [cond-mat.str-el] 27 Dec 2016

Light-induced fractional quantum Hall phases in graphene

Areg Ghazaryan,[1] Michael J. Gullans,[2,3] Pouyan Ghaemi,[1,4] and Mohammad Hafezi[2,5]

[1]*Department of Physics, City College, City University of New York, New York, NY 10031, USA*
[2]*Joint Quantum Institute, NIST and University of Maryland, College Park, MD 20742, USA*
[3]*Joint Center for Quantum Information and Computer Science, University of Maryland, College Park, Maryland 20742, USA*
[4]*Department of Physics, Grad. Center, City University of New York, New York, NY 10016, USA*
[5]*Department of Electrical Engineering and Institute for Research in Electronics and Applied Physics, University of Maryland, College Park, MD 20742, USA*

We show how to realize two-component fractional quantum Hall phases in monolayer graphene by optically driving the system. A laser is tuned into resonance between two Landau levels of graphene and acts as a effective tunneling term between these states. We study systems with small number of electrons for filling factor 2/3 using exact-diagonalization. When the lower state is the first Landau level, we find that tuning the effective tunneling amplitude causes the system to undergo a phase transition from a spin-singlet phase to a particle-hole conjugate 1/3 Laughlin phase of the antisymmetric optical dressed states. This phase transition can be traced to the presence of additional cross interaction terms that arise in the rotating wave approximation. These results pave the way towards the realization of new phases, as well as the control of phase transitions, in graphene quantum Hall systems using optical fields and integrated photonic structures.

The fractional quantum Hall (FQH) effect is a fascinating phenomena in condensed matter physics, whereby electron-electron interaction fully determine the behavior of the system [1–3]. While initial considerations focused on systems with no internal degrees of freedom, later it was realized that the electron spin plays an important role for several filling factors [4–7], which was confirmed experimentally [8, 9]. More generally, multicomponent FQH phases [10] occur in numerous systems, where the role of the internal degree of freedom is ascribed to subbands, such as in wide quantum wells [11–14], layers, such as in double quantum wells [15, 16], or the valley quantum number, such as in AlAs quantum well [17] and graphene [18–20]. In particular, there has been much effort towards engineering various system parameters, such as tunneling, to realize different FQH states. However, these approaches can add unwanted side effects, and therefore, it is desirable to investigate other control methods.

At the same time, there has been many theoretical [21–24] and experimental [25–28] studies of the interaction of light with quantum Hall states of graphene. In particular, due the linear dispersion in graphene, the Landau levels (LL) are not equidistant, unlike semiconductors with a parabolic dispersion [29]. This makes it possible to selectively couple LLs with resonant light. More recently, FQH phases in integrated GaAs quantum well-cavity structures have also been explored experimentally [30].

In this Letter, we explore the possibility of using light to control multicomponent FQH phases of graphene. Resonant excitation by light results in an effective tunneling between two LL, with a rate proportional to the amplitude of the electric field. The optical driving results in the formation of dressed states of LL orbits. Consequently, the Coulomb interaction terms between different LLs, which are usually ignored due to the negligible population of the higher LLs, become important. These terms come in two categories: (1) direct terms, which are the counterpart of inter-layer interaction in bilayer systems [31–33], and (2) cross terms, which are absent in conventional bilayer systems. The latter terms further turn out to be crucial in understanding how our system deviates from the usual bilayer systems. We numerically study the case of $\nu = 2/3$ filling on a torus and find that, when the effective tunneling rate is large, the system forms a Laughlin state out of the dressed LL orbitals. This is the case for all values of tunneling we considered for $\mathrm{LL}_0 - \mathrm{LL}_1$ transitions. In contrast, for the $\mathrm{LL}_1 - \mathrm{LL}_2$ transition with a small effective tunneling rate, the cross terms in the Coulomb interaction compete with the energy separation of the dressed states and force the system into a many-body singlet state. This state is the result of the cross Coulomb interaction terms, and therefore, has infinitesimal overlap with the usual bilayer singlet [31, 34, 35].

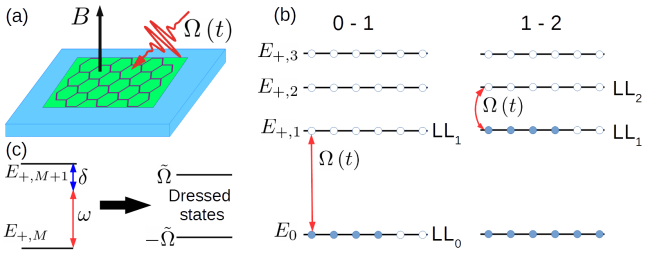

FIG. 1: (a) A single layer of of graphene driven by a light with Rabi frequency coupling Ω. (b) LL structure with partial filling and optical transitions between $0-1$ and $1-2$ states. (c) Formation of the dressed states due to the light coupling between two LLs.

We consider a monolayer of graphene under perpendicular magnetic field which is optically driven. The low-energy Hamiltonian of graphene has the familiar form [29]

$$\mathcal{H}_0^{\xi} = v_{\rm F}\left(\xi\Pi_x\sigma_x + \Pi_y\sigma_y\right), \tag{1}$$

where ξ is the valley index, σ_i are Pauli matrices acting on sublattice spinor and $\mathbf{\Pi} = \mathbf{p} + e\mathbf{A}(\mathbf{r})/c$ is the kinetic momentum (electron charge being $-e$, $\hbar = 1$). Here $\mathbf{A}(\mathbf{r})$ is the static vector potential which is responsible for Landau quantization and we use Landau gauge in this work, namely $\mathbf{A}(\mathbf{r}) = -By\hat{\mathbf{x}}$. The two-component solution of Hamiltonian (1) can be expressed as $(\psi_A, \psi_B)^T$, where ψ_A and ψ_B are the wave functions of sublattices A and B, respectively. In this spinor representation, the wave function of (1) in valley K is

$$\Psi^K_{\gamma,n,k}(x,y) = \begin{pmatrix} -\gamma C_n^- \phi_{n-1,k}(x,y) \\ C_n^+ \phi_{n,k}(x,y) \end{pmatrix}, \tag{2}$$

where $C_n^{\pm} = \sqrt{\left(1 \pm \delta_{n,0}\right)/2}$. $\gamma = \pm$ labels the states with positive and negative energy, namely $E_{\gamma,n} = \gamma\omega_{\rm c}\sqrt{n}$, where $\omega_{\rm c} = \sqrt{2}v_{\rm F}/l_B$ and $l_B = \sqrt{c/eB}$ is the magnetic length. In (2) $\phi_{n,k}(x,y)$ are the LL wave functions with parabolic dispersion, where n is the LL index and k labels the momentum in x direction. In this work we consider a torus geometry and therefore, LL wave functions with parabolic dispersion, after imposing periodic boundary conditions (PBC), will have the form [1]

$$\begin{aligned}\phi_{n,j}(x,y) =& C_n \sum_{m=-\infty}^{\infty} e^{\frac{i}{l_B^2}(Y_j - mL_y)x} \\ & \times e^{-\frac{\left(y+mL_y-Y_j\right)^2}{2l_B^2}} H_n\left(\frac{y+mL_y-Y_j}{l_B}\right),\end{aligned} \tag{3}$$

where $C_n = \left(L_x\sqrt{\pi}l_B 2^n n!\right)^{-\frac{1}{2}}$, $Y_j = kl_B^2 = 2\pi j l_B^2/L_x$. Here L_x and L_y describe the size of magnetic translation unit cell, j is an integer, which takes the values $0, 1\cdots N_s - 1$, $N_s = L_xL_y/2\pi l_B^2$ describing the degeneracy of each LL. j is the quantum number characterizing momentum in x direction. For simplicity, we disregard the spin of the electrons and consider only the electrons in K valley.

Taking the Fermi energy of the system to lie in LL_M in conduction band and the frequency of the optical drive near resonant with the transition between LL_M and LL_{M+1} (Fig. 1 (a,b)), we can approximate the light-matter interaction with the Hamiltonian

$$\mathcal{H}_{\rm int} = \sum_{j,j'} \Omega_{j,j'}(t) c^{\dagger}_{M+1,j} c_{M,j'} + \text{H.c.}, \tag{4}$$

where $c^{\dagger}_{M,j}$ and $c_{M,j}$ are the creation and annihilation operators in LL_M with the momentum quantum number j. For simplicity, we assume a plane wave drive, which acts uniformly on all orbitals: $\Omega_{j,j'}(t) = 2\Omega\delta_{j,j'}\cos(\omega t)$, where ω is the drive frequency, and we take the Rabi frequency Ω to be real. We take the light to be slightly detuned from the resonance, so that $\delta = E_{+,M+1} - E_{+,M} - \omega$. The single particle Hamiltonian has the form

$$H_d = \frac{\delta}{2}\tau_z + \Omega\tau_x, \tag{5}$$

where τ_i are the Pauli matrices, which act on a spinor composed of LL wave functions involved in an optical transition. In the Landau gauge, the Hamiltonian is diagonal in terms of the momentum in x-direction. The eigenvalues of this single particle Hamiltonian are the dressed states with the energy $\pm\tilde{\Omega} = \pm\sqrt{\frac{\delta^2}{4} + \Omega^2}$ (Fig. 1 (c)). We consider the weak excitation limit, where $\Omega \ll E_{+,M+1} - E_{+,M}$, and use the rotating-wave approximation (RWA) to eliminate time-dependent terms in both the single-particle terms and the Coulomb interactions in the Hamiltonian, i.e., counter-rotating terms proportional to $e^{iO(\omega)t}$. This approximation is expected to have the greatest validity in the limit of $(\Omega, e^2/\epsilon l_B) \ll \omega$. The second quantized Hamiltonian in the rotating frame is obtained by performing a unitary transformation with the operator: $U = \exp\left[-\frac{i}{2}\omega t\sum_j\left(c^{\dagger}_{M,j}c_{M,j} - c^{\dagger}_{M+1,j}c_{M+1,j}\right)\right]$ which transforms the full Hamiltonian to

$$\begin{aligned}\tilde{\mathcal{H}} =& \sum_j \frac{\delta}{2}\left(c^{\dagger}_{M+1,j}c_{M+1,j} - c^{\dagger}_{M,j}c_{M,j}\right) \\ & + \sum_{\substack{n_1,n_2\\n_3,n_4}}\sum_{\substack{j_1,j_2\\j_3,j_4}} A^{n_1,j_1,n_2,j_2}_{n_3,j_3,n_4,j_4}\delta_{n_1+n_2,n_3+n_4}c^{\dagger}_{n_1,j_1}c^{\dagger}_{n_2,j_2} \\ & \times c_{n_3,j_3}c_{n_4,j_4} + \sum_j\left(\Omega c^{\dagger}_{M,j}c_{M+1,j} + \text{H.c.}\right),\end{aligned} \tag{6}$$

where, in contrast to earlier work [1, 36], we represent the Coulomb matrix elements using Haldane pseudopotentials [37]

$$\begin{aligned}A^{n_1,j_1,n_2,j_2}_{n_3,j_3,n_4,j_4} =& \delta'_{j_1+j_2,j_3+j_4}\sum_{m=0}^{\infty}\frac{V_m^{n_1n_2n_3n_4}}{N_s} \\ & \times \sum_{\mathbf{q}}{}' \delta'_{j_1-j_4,q_xL_x/2\pi} e^{iq_y(Y_{j_1}-Y_{j_3})} e^{-\frac{q^2l_B^2}{2}} L_m(q^2l_B^2),\end{aligned} \tag{7}$$

where primed summation excludes $\mathbf{q} = 0$ term and primed Kronecker δ' is defined mod N_s. The $V_m^{n_1n_2n_3n_4}$ are Haldane pseudopotentials defined in Supplementary material. The form of the Hamiltonian Eq.(6) is similar to bilayer FQH system with interlayer separation $d = 0$ considered previously [31], where LL index corresponds to layer index and the light coupling plays the role of effective tunneling between the layers.

Despite these similarities, there are also differences between the two systems. In our case, the Coulomb interaction, being different in each LL, breaks the SU(2)

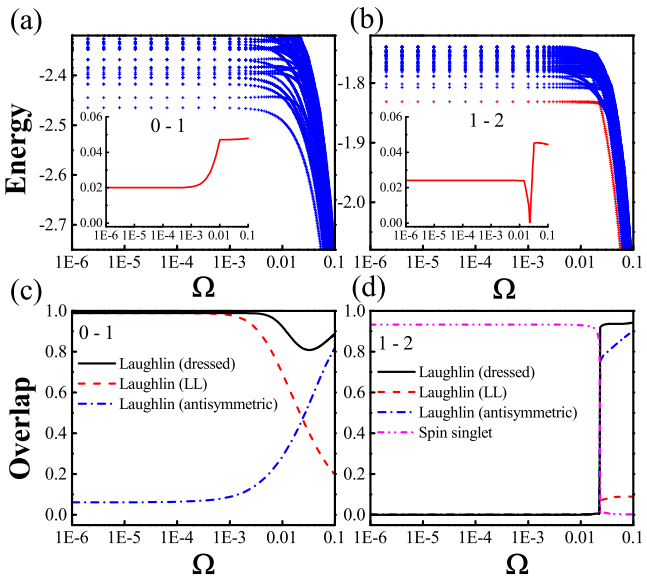

FIG. 2: The dependence of the low lying energy levels on the effective tunneling Ω for different transitions $0-1$ (a) and $1-2$ (b). Insets show the dependence of the gap between ground and first excited state on Ω. The dependence of the overlap between trial wave functions and numerically exact ground state on effective tunneling Ω for the case of transition $0-1$ (c) and $1-2$ (d). All energies are in units of $e^2/\epsilon l_B$ and for all figures $\delta = 0.02$.

pseudo-spin symmetry present in the conventional bilayer case. More specifically, in RWA, the energy-conserving Coulomb interaction terms are the ones with equal initial and final energies which results in the presence of $\delta_{n_1+n_2,n_3+n_4}$ in Eq.(6). Since we are limiting the system to two LLs, we can write $\delta_{n_1+n_2,n_3+n_4}$ as $\delta_{n_1,n_4}\delta_{n_2,n_3}$ or $\delta_{n_1,n_3}\delta_{n_2,n_4}$. We denote the first term as direct which is similar to the density-density type interaction between the LLs, whereas the second term is designated as cross term and is similar to an exchange type interaction between the LLs (see Supplementary Material). Note that in conventional bilayer systems the layer index acts as a pseudo-spin and only direct type interactions between the layers are present. Due to the fact that in conventional bilayer systems the exchange type interaction is only present for intra-layer interactions, it was initially supposed that FQHE phases should be pseudo-spin polarized, which was proven to be wrong by exact-diagonalization [5–7] and experimental studies [8, 9]. The presence of inter-layer cross interaction terms in our case nominally makes the competition between pseudo-spin polarized and unpolarized phases even more important, but it competes with the SU(2) symmetry breaking. The competition between the SU(2) symmetry breaking and inter LL cross interaction terms will be analyzed below.

We have performed exact-diagonalization studies of the system containing eight electrons with filling factor $\nu = N_e/N_s = 2/3$ on torus geometry using magnetic translation symmetry [1, 38]. In the absence of light, the FQH phases in graphene are well studied [39–43] both in single-component and multicomponent regimes. Recently, bilayer 2/3 filling system has received renewed interest because of the possibility of obtaining additional non-Abelian phases by engineering special type of interaction potentials [44–46]. We have considered the system to initially occupy the LL_0 or LL_1 and then optically couple these levels to LL_1 and LL_2 respectively. We denote these two cases as the $0-1$ and $1-2$ transitions, respectively (Fig. 1 (b)). In the calculations, we take the unit of the energy to be $e^2/\epsilon l_B$. All calculations are performed for non-zero detuning ($\delta = 0.02$) to rule out singular behavior associated with driving exactly on resonance. Due to the computational complexity, we disregard LL mixing to other levels not involved in the optical transition, which is a good approximation for graphene placed on a substrate [47, 48].

In Fig. 2, the dependence of the low lying energy levels and overlap with trial wave functions on the effective tunneling Ω is presented for different transitions $0-1$ and $1-2$. It is clear from the figure that these two cases demonstrate different behavior, as we change the tunneling Ω. It should be noted that for both transitions and for all phases observed in the system the obtained energy levels are triple degenerate. For the $0-1$ case, there is no ground state crossing and the system has finite gap for all values of Ω, as shown in Fig. 2(a). Therefore, the system always remains in the same phase, which is the particle-hole conjugate 1/3 Laughlin phase. This claim is further justified by analyzing the overlap between several trial wave functions and the obtained exact wave functions, for different values of Ω, as shown in Fig. 2(c). For particle-hole conjugate 1/3 Laughlin state, we consider three different bases: (1) LL basis, when all the electrons reside in initial LL, (2) the dressed state basis, when all electrons reside in lower energy dressed orbitals with energy $-\tilde{\Omega}$, i.e., a Laughlin state formed of lower eigenstates of Eq. (5) orbitals: $|\pm, j\rangle \propto \left(\delta \pm \sqrt{\delta^2 + 4\Omega^2}\right)|M+1, j\rangle + 2\Omega|M, j\rangle$, (3) symmetric-antisymmetric basis, when all electrons reside in the antisymmetric state, i.e., lower energy dressed orbital when $\Omega \gg \delta$, $|-, j\rangle = \frac{1}{\sqrt{2}}(-|M+1, j\rangle + |M, j\rangle)$. For weak tunnelings ($\Omega \ll \delta$), the state remains polarized in lowest LL system and has a large overlap with the particle-hole conjugate 1/3 Laughlin state. In this regime, the dressed states coincides with orbitals in the absence of the light coupling ($|-, j\rangle \approx |M, j\rangle$). As the tunneling increases, the dressed state acquires a bigger component from the opposite orbital, however, we observe that the overlap with the dressed Laughlin state remains large. In the strong tunneling limit ($\Omega \gg \delta$), the dressed orbital coincide with symmetric and antisymmetric states and the system develops a large overlap with antisymmetric wave function. In summery, for $0-1$ case, the system remains in a particle-hole con-

jugate Laughlin 1/3 phase, but it makes the transition from being polarized in one LL to being polarized in an antisymmetric state, a feature which is captured by the dressed state picture. The fact that gap does not close during this transition shows that these two particle-hole conjugate 1/3 phases can be adiabatically connected to one another without destroying FQH phase.

The situation is different for the transition $1-2$. As shown in Fig. 2(b), there is a ground state crossing at $\Omega_c \approx 0.02$, and two different phases are observed for this case. We claim that the phase observed for $\Omega < \Omega_c$ is the spin-singlet phase, where the expectation value of the collective spin operator associated with the orbitals is zero (see Supplementary Material). For higher values of $\Omega > \Omega_c$, there is a phase transition from the spin-singlet phase to a particle-hole conjugate 1/3 Laughlin phase of the antisymmetric state. Although a similar phase transition was obtained for the conventional bilayer system [31, 44, 46], as noted above, the interaction in this system is not SU(2) symmetric, and therefore, the observation of spin-singlet phase has a different origin. The presence of the spin-singlet phase is attributed to the inter-layer interaction cross terms, which are absent in usual bilayer system. We have further checked that this phase transition does not happen when the cross terms are artificially switched off.

The above claims are justified by the investigation of the populations of LLs and symmetric and antisymmetric states for both $0-1$ and $1-2$ transitions (see Supplementary Material). Due to the fact that full wave function can have even parity for the interchange of particle coordinates with different LL indices, V_0 pseudopotentials are responsible for different physics observed for two transitions. For $0-1$ transition, V_0 pseudopotential corresponding to direct terms is considerably larger compared to $1-2$ transition. This direct term competes with the cross term and hinders the formation of the singlet phase for $0-1$ transition (see Supplementary Material).

In the large tunneling limit ($\Omega \gg \delta$), the situation for $1-2$ is similar to $0-1$ case. Specifically, since the single particle orbits energy gap is large $2\tilde{\Omega}$, compared to the Coulomb energy, the state remains polarized, and the overlap with dressed Laughlin state is large, as shown in Fig. 2(d). However, when the tunneling decreases, the cross terms of the interaction force the system to form a singlet. In the overlap calculation for the spin-singlet trial wave function, we used a model interaction potential similar to the one used for Jain's spin-singlet state [3, 49, 50]. In particular, in the interaction potential, we have kept only the V_0 and V_1 Haldane pseudopotentials and set them equal to 1. For the cross terms of the interaction, we choose $V_0 = 6.35$ which gave the highest overlap of 93 %. As can be seen from Fig. 2 (d), the overlap with spin-singlet trial wave function is almost constant for small $\Omega < \Omega_c$ and abruptly drops to zero after the phase transition for $\Omega > \Omega_c$. Due to the presence of cross terms, the obtained singlet state has infinitesimal overlap with Jain's spin-singlet state, and therefore, is a different many-body singlet state, which deserves further analytical investigations.

In this work, we have assumed that the electronic system thermalizes to the ground state in the rotating frame of the optical drive field. To estimate the validity of this approximation, we have to compare the timescale for relaxation of the optically excited Landau levels to the timescale for thermalization of the electronic system with the lattice. The carrier lifetime of optically excited Landau levels has contributions from optical relaxation, phonon relaxation, and Auger scattering into other Landau levels [51]. In Ref. [52], it was measured at moderate magnetic fields in epitaxial graphene samples to be roughly 10 - 20 ps. Although, one expects longer lifetimes in higher quality graphene samples suitable to observe the FQH effect, we can use this as an upper bound on the relaxation rate. In our units of Coulomb interaction $e^2/\epsilon l_B$, this timescale translates to roughly 10^{-3} to 10^{-4}, depending on the magnetic field. We roughly estimate the thermalization time by the size of the many-body gap in the spectrum, which, from Fig. 2, is on the order of 10^{-2}. As a result, there is a large separation of timescales between the thermalization and carrier relaxation, which allows our system to remain in the rotating frame ground states before carrier relaxation. In our case, the Laughlin state of the driven regime can be adiabatically connected to the Laughlin state of a non-driven regime. Therefore, one can adiabatically prepare the system by slowly turning on the light field. In contrast, the singlet state can not be connected to the non-driven regime, which makes the thermalization problem particularly relevant. A more detailed study of the thermalization dynamics in this regime is beyond the scope of the present work; however, it is worth noting that there has been recent progress in understanding of thermalization of driven isolated systems [53–55] and also thermalization of Floquet systems coupled to a bath [56, 57]. Most importantly, it has been pointed out that electron-phonon interaction and specific Fermi reservoirs could lead to thermalization of the system in the rotating frame, in the long time steady-state limit [57].

In conclusion, we have considered single layer graphene sheet in the FQH regime with an externally applied optical field that is resonant between two LLs of graphene. We showed that a two-component FQH system can be constructed with two LLs that are brought into resonance with the light, where the external light field plays the role of tunneling between two layers. For the $0-1$ case, the system is always in particle-hole conjugate Laughlin 1/3 phase: as the tunneling rate increases, the system changes from being polarized in LL to being polarized in the state of antisymmetric superposition of LLs. In contrast, for the transition $1-2$, we were able to demonstrate the phase transition between spin-singlet and particle-

hole conjugate Laughlin 1/3 phase for a critical value of Ω_c. The spin-singlet phase and the associated phase transition observed for the $1-2$ case arise from the cross terms of the inter LL interaction, which are absent in usual multicomponent systems. Similar FQH phases induced by light in other 2D materials with Dirac bands, such as monolayer transition metal dichalcogenides [58, 59] will be subject of future works. This study gives new impetus towards experimental realization of multicomponent FQH states and *in situ* control of the phase transition using externally applied optical fields.

We acknowledge fruitful comments by S. Simon, E. Demler, K. Seetharam and S. Das Sarma. This research was supported under National Science Foundation Grants EFRI-1542863, PFC at the Joint Quantum Institute, CNS-0958379, CNS-0855217, ACI-1126113 and the City University of New York High Performance Computing Center at the College of Staten Island, and AFOSR-MURI FA95501610323, Sloan Fellowship, YIP-ONR.

[1] T. Chakraborty and P. Pietiläinen, *The Quantum Hall Effects* (Springer, New York, 1995).
[2] R. E. Prange and S. M. Girvin, *The Quantum Hall Effects* (Springer-Verlag, New York, 1990).
[3] J. K. Jain, *Composite Fermions* (Cambridge University Press, Cambridge, 2007).
[4] B. I. Halperin, Helvetica Physica Acta **56**, 75 (1983).
[5] T. Chakraborty and F. C. Zhang, Phys. Rev. B **29**, 7032 (1984).
[6] F. C. Zhang and T. Chakraborty, Phys. Rev. B **30**, 7320 (1984).
[7] X. C. Xie, Y. Guo, and F. C. Zhang, Phys. Rev. B **40**, 3487 (1989).
[8] J. P. Eisenstein, H. L. Stormer, L. N. Pfeiffer, and K. W. West, Phys. Rev. Lett. **62**, 1540 (1989).
[9] J. P. Eisenstein, H. L. Stormer, L. N. Pfeiffer, and K. W. West, Phys. Rev. B **41**, 7910 (1990).
[10] S. M. Girvin and A. H. MacDonald, in *The Perspectives in Quantum Hall Effects*, edited by S. D. Sarma and A. Pinczuk (John Wiley & Sons Inc., New York, 1997) Chap. 5, pp. 161–224.
[11] Y. W. Suen, H. C. Manoharan, X. Ying, M. B. Santos, and M. Shayegan, Phys. Rev. Lett. **72**, 3405 (1994).
[12] T. S. Lay, T. Jungwirth, L. Smrčka, and M. Shayegan, Phys. Rev. B **56**, R7092 (1997).
[13] J. Shabani, Y. Liu, M. Shayegan, L. N. Pfeiffer, K. W. West, and K. W. Baldwin, Phys. Rev. B **88**, 245413 (2013).
[14] Y. Liu, S. Hasdemir, J. Shabani, M. Shayegan, L. N. Pfeiffer, K. W. West, and K. W. Baldwin, Phys. Rev. B **92**, 201101 (2015).
[15] J. P. Eisenstein, G. S. Boebinger, L. N. Pfeiffer, K. W. West, and S. He, Phys. Rev. Lett. **68**, 1383 (1992).
[16] Y. W. Suen, L. W. Engel, M. B. Santos, M. Shayegan, and D. C. Tsui, Phys. Rev. Lett. **68**, 1379 (1992).
[17] N. C. Bishop, M. Padmanabhan, K. Vakili, Y. P. Shkolnikov, E. P. D. Poortere, and M. Shayegan, Phys. Rev. Lett. **98**, 266404 (2007).
[18] C. R. Dean, A. F. Young, P. Cadden-Zimansky, L. Wang, H. Ren, K. Watanabe, T. Taniguchi, P. Kim, J. Hone, and K. L. Shepard, Nature Physics **7**, 693 (2011).
[19] B. E. Feldman, B. Krauss, J. H. Smet, and A. Yacoby, Science **337**, 1196 (2012).
[20] B. E. Feldman, A. J. Levin, B. Krauss, D. A. Abanin, B. I. Halperin, J. H. Smet, and A. Yacoby, Phys. Rev. Lett. **111**, 076802 (2013).
[21] M. Furchi, A. Urich, A. Pospischil, G. Lilley, K. Unterrainer, H. Detz, P. Klang, A. M. Andrews, W. Schrenk, G. Strasser, and T. Mueller, Nano Lett. **12**, 2773 (2012).
[22] D. Hagenmüller and C. Ciuti, Phys. Rev. Lett. **109**, 267403 (2012).
[23] L. Chirolli, M. Polini, V. Giovannetti, and A. H. MacDonald, Phys. Rev. Lett. **109**, 267404 (2012).
[24] F. M. D. Pellegrino, L. Chirolli, R. Fazio, V. Giovannetti, and M. Polini, Phys. Rev. B **89**, 165406 (2014).
[25] M. Byszewski, B. Chwalisz, D. K. Maude, M. L. Sadowski, M. Potemski, T. Saku, Y. Hirayama, S. Studenikin, D. G. Austing, A. S. Sachrajda, and P. Hawrylak, Nat. Phys. **2**, 239 (2006).
[26] Z. Jiang, E. A. Henriksen, L. C. Tung, Y. J. Wang, M. E. Schwartz, M. Y. Han, P. Kim, and H. L. Stormer, Phys. Rev. Lett. **98**, 197403 (2007).
[27] M. Orlita, C. Faugeras, P. Plochocka, P. Neugebauer, G. Martinez, D. K. Maude, A. L. Barra, M. Sprinkle, C. Berger, W. A. de Heer, and M. Potemski, Phys. Rev. Lett. **101**, 267601 (2008).
[28] M. Orlita, C. Faugeras, R. Grill, A. Wysmolek, W. Strupinski, C. Berger, W. A. de Heer, G. Martinez, and M. Potemski, Phys. Rev. Lett. **107**, 216603 (2011).
[29] M. O. Goerbig, Rev. Mod. Phys. **83**, 1193 (2011).
[30] S. Smolka, W. Wuester, F. Haupt, S. Faelt, W. Wegscheider, and A. Imamoglu, Science **346**, 332 (2014).
[31] I. A. McDonald and F. D. M. Haldane, Phys. Rev. B **53**, 15845 (1996).
[32] K. Moon, H. Mori, K. Yang, S. M. Girvin, A. H. MacDonald, L. Zheng, D. Yoshioka, and S.-C. Zhang, Phys. Rev. B **51**, 5138 (1995).
[33] K. Yang, K. Moon, L. Belkhir, H. Mori, S. M. Girvin, A. H. MacDonald, L. Zheng, and D. Yoshioka, Phys. Rev. B **54**, 11644 (1996).
[34] X. G. Wu, G. Dev, and J. K. Jain, Phys. Rev. Lett. **71**, 153 (1993).
[35] J. E. Moore and F. D. M. Haldane, Phys. Rev. B **55**, 7818 (1997).
[36] D. Yoshioka, B. I. Halperin, and P. A. Lee, Phys. Rev. Lett. **50**, 1219 (1983).
[37] J.-S. Jeong and K. Park, Phys. Rev. B **91**, 195119 (2015).
[38] F. D. M. Haldane, Phys. Rev. Lett. **55**, 2095 (1985).
[39] T. Chakraborty and V. Apalkov, in *Physics of Graphene*, edited by H. Aoki and M. S. Dresselhaus (Springer, New York, 2013) Chap. 8, pp. 251–300.
[40] T. Chakraborty and V. M. Apalkov, Solid State Commun. **175**, 123 (2013).
[41] M. O. Goerbig and N. Regnault, Phys. Rev. B **75**, 241405 (2007).
[42] Z. Papić, M. O. Goerbig, and N. Regnault, Solid State Commun. **149**, 1056 (2009).
[43] C. Tőke and J. K. Jain, Phys. Rev. B **75**, 245440 (2007).
[44] S. Geraedts, M. P. Zaletel, Z. Papić, and R. S. K. Mong, Phys. Rev. B **91**, 205139 (2015).
[45] Z. Liu, A. Vaezi, K. Lee, and E.-A. Kim, Phys. Rev. B **92**, 081102 (2015).

[46] M. R. Peterson, Y.-L. Wu, M. Cheng, M. Barkeshli, Z. Wang, and S. D. Sarma, Phys. Rev. B **92**, 035103 (2015).
[47] M. R. Peterson and C. Nayak, Phys. Rev. B **87**, 245129 (2013).
[48] M. R. Peterson and C. Nayak, Phys. Rev. Lett. **113**, 086401 (2014).
[49] L. Belkhir, X. G. Wu, and J. K. Jain, Phys. Rev. B **48**, 15245 (1993).
[50] N. Moran, A. Sterdyniak, I. Vidanović, N. Regnault, and M. V. Milovanović, Phys. Rev. B **85**, 245307 (2012).
[51] H. Funk, A. Knorr, F. Wendler, and E. Malic, Phys. Rev. B **92**, 205428 (2015).
[52] M. Mittendorff, F. Wendler, E. Malic, A. Knorr, M. Orlita, M. Potemski, C. Berger, W. A. de Heer, H. Schneider, M. Helm, and S. Winnerl, Nat. Phys. **11**, 75 (2015).
[53] A. Lazarides, A. Das, and R. Moessner, Phys. Rev. Lett. **112**, 150401 (2014).
[54] L. D'Alessio and M. Rigol, Phys. Rev. X **4**, 041048 (2014).
[55] P. Ponte, A. Chandran, Z. Papic, and D. A. Abanin, Annals of Physics **353**, 196 (2015).
[56] H. Dehghani, T. Oka, and A. Mitra, Phys. Rev. B **90**, 195429 (2014).
[57] K. I. Seetharam, C.-E. Bardyn, N. H. Lindner, M. S. Rudner, and G. Refael, Phys. Rev. X **5**, 041050 (2015).
[58] D. Xiao, G.-B. Liu, W. Feng, X. Xu, and W. Yao, Phys. Rev. Lett. **108**, 196802 (2012).
[59] Z. Wang, J. Shan, and K. F. Mak, Nature Nanotech. (2016), 10.1038/nnano.2016.213.

Supplementary online material for the paper Light-induced fractional quantum Hall phases in graphene

DEFINITION OF INTERACTION TERMS

In this section we elaborate in more detail about the notation used to denote different interaction terms in the main text. The interaction matrix elements are defined as

$$A_{n_1,j_1,n_2,j_2,n_3,j_3,n_4,j_4} = \frac{1}{2}\int_0^{L_x} dx_1 \int_0^{L_y} dy_1 \int_0^{L_x} dx_2 \int_0^{L_y} dy_2 \Psi^\dagger_{n_1,j_1}(x_1,y_1)\Psi^\dagger_{n_2,j_2}(x_2,y_2) \times V(|\mathbf{r_1}-\mathbf{r_2}|)\Psi_{n_3,j_3}(x_2,y_2)\Psi_{n_4,j_4}(x_1,y_1), \tag{S1}$$

where $\Psi^\dagger_{n,j}(x,y)$ are single particle wave function of graphene defined by (2) of main text. Due to the fact that we have additional $\delta_{n_1+n_2,n_3+n_4}$ term coming from RWA, the possible nonzero terms of interaction are presented in table S1, where it is assumed that $n_1 \neq n_2$.

According to (6) of the main text the interaction matrix elements contain the terms $\delta'_{j_1+j_2,j_3+j_4}$ and $\delta'_{j_1-j_4,q_xL_x/2\pi}$, where the primed Kronecker δ' is defined mod N_s. For simplicity lets ignore the primes on Kronecker delta and treat them as usual Kronecker delta functions. Lets also denote $\alpha = q_xL_x/2\pi$. Then the interaction matrix elements are non-zero if $j_1 = j_4+\alpha$ and $j_2 = j_3-\alpha$. Using this simplification the notation of the interaction terms becomes similar to the one used in Hartree-Fock theory [1]. For inter LL interaction terms of line (2) of table S1 the case when $j_1 = j_4$ and $j_2 = j_3$ corresponds to density-density type interaction. Notice that although this matrix element corresponds to $q_x = 0$ it is non-zero, because for non-zero q_y terms in the sum of (6) in the main text. Therefore, even for general $q_x \neq 0$ or the case of primed Kronecker delta the terms on line (2) of table S1 are similar to density-density type interaction and we denote them as direct interaction terms. Similarly for the case of line (3) of table S1 the matrix elements are similar to exchange type of interaction, although again due to the degenerate state manifold the condition of $j_1 = j_3$ and $j_2 = j_4$ is not the only possibility, and we denote them as cross interaction terms. In summary this characterization of the inter LL interaction terms is only based on LL indices. Obviously, for intra LL interaction this kind of separation is not possible, therefore, we have denoted them with the general intra LL interaction terms in line (1) of table S1.

POPULATION NUMBERS OF THE LEVELS

In this section we analyze the dependence of population in both LLs and symmetric and antisymmetric dressed states (defined as $|\pm, j\rangle = \frac{1}{\sqrt{2}}(\pm|M+1,j\rangle + |M,j\rangle)$) on effective tunneling Ω, which confirms once more the observed phases for both transitions $0-1$ and $1-2$. The corresponding dependences are shown in Fig. S1. In accordance with the claims made in the main text, for the $0-1$ transition (Fig. S1 (a)), all electrons are located at the initial LL_0 for small Ω, while, for large Ω, the system almost reaches to equal population in both LLs. As for the populations in the basis of symmetric and antisymmetric dressed states valid for $\Omega \gg \delta$, for high values of Ω, almost all the electrons are located in the state of antisymmetric superposition of LLs. As can be seen from Fig. S1 (b) for the case of transition $1-2$ for small values of Ω both LLs and symmetric and antisymmetric states are equally populated, which is the indication of spin-singlet state. With the increase of Ω there is jump in the population dependences in accordance with phase transition and the system switches to the phase where both LLs are equally populated, but all electrons reside in antisymmetric superposition of LLs. Therefore this indicates once more that there is a phase transition from spin-singlet phase into particle-hole conjugate 1/3 Laughlin phase for transition $1-2$.

TABLE S1: Notation of the different interaction terms used in the main text

(1)	$A_{n,j_1,n,j_2,n,j_3,n,j_4} c^\dagger_{n,j_1} c^\dagger_{n,j_2} c_{n,j_3} c_{n,j_4}$	Intra LL interaction for LL_n
(2)	$A_{n_1,j_1,n_2,j_2,n_2,j_3,n_1,j_4} c^\dagger_{n_1,j_1} c^\dagger_{n_2,j_2} c_{n_2,j_3} c_{n_1,j_4}$	Inter LL direct interaction terms between LL_{n_1} and LL_{n_2}
(3)	$A_{n_1,j_1,n_2,j_2,n_1,j_3,n_2,j_4} c^\dagger_{n_1,j_1} c^\dagger_{n_2,j_2} c_{n_1,j_3} c_{n_2,j_4}$	Inter LL cross interaction terms between LL_{n_1} and LL_{n_2}

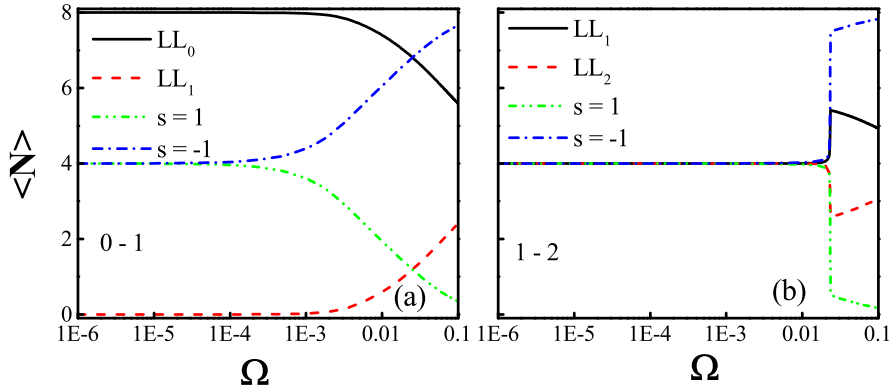

FIG. S1: The dependence of the population in both LLs and symmetric and antisymmetric states in the ground state of the system on effective tunneling Ω for the case of transition $0-1$ (a) and $1-2$ (b) for $\delta = 0.02$.

EXPECTATION VALUES OF SPIN OPERATORS

In this section we consider the expectation values of total spin operators defined as

$$S_x = \frac{1}{2N_e} \sum_{j=0}^{N_s-1} \left(c^\dagger_{M,j} c_{M+1,j} + c^\dagger_{M+1,j} c_{M,j} \right), \tag{S2}$$

$$S_y = -\frac{i}{2N_e} \sum_{j=0}^{N_s-1} \left(c^\dagger_{M,j} c_{M+1,j} - c^\dagger_{M+1,j} c_{M,j} \right), \tag{S3}$$

$$S_z = \frac{1}{2N_e} \sum_{j=0}^{N_s-1} \left(c^\dagger_{M,j} c_{M,j} - c^\dagger_{M+1,j} c_{M+1,j} \right). \tag{S4}$$

The dependence of the S_x and S_z on effective tunneling Ω is shown in Fig. S2 for transitions $0-1$ (a) and $1-2$ (b). The expectation value of S_y is always zero. In accordance with the claims made in the main text for transition $0-1$ for small values of Ω S_z has maximum value and the system is spin polarized into lowest LL with $1/3$ particle-hole conjugate Laughlin phase. With the increase of Ω the system total spin rotates in the xz plane and for $\Omega \gg \delta$ it gets polarized opposite to x direction still being characterized with the same phase. In dressed states basis this corresponds to the situation when the system is always polarized into lower dressed state. For transition $1-2$ the situation is different as was also noted in the main text. For small values of Ω all components of spin are zero, and therefore, the system is in spin-singlet phase. Increasing Ω results in the increase of the gap between two dressed states and at some value of Ω this gap becomes comparable with Coulomb interaction and phase transition is observed. After phase transition the system gets polarized into antisymmetric dressed state with $1/3$ particle-hole conjugate Laughlin phase. As for the case of $0-1$ transition, for $1-2$ for $\Omega \gg \delta$ the expectation value of S_x reaches maximum value and total spin is aligned opposite to x direction.

HALDANE PSEUDOPOTENTIALS

In this section we review the appropriate Haldane pseudopotentials and the way they impact the observed phases for both transitions. Haldane pseudopotentials are defined as [2]

$$V_m^{n_1 n_2 n_3 n_4} = \frac{1}{4\pi^2} \int d^2 q V(q) e^{\frac{-q^2 l_B^2}{2}} L_m(q^2 l_B^2) \mathcal{F}_{n_1,n_4}(\mathbf{q}) \mathcal{F}_{n_2,n_3}(-\mathbf{q}), \tag{S5}$$

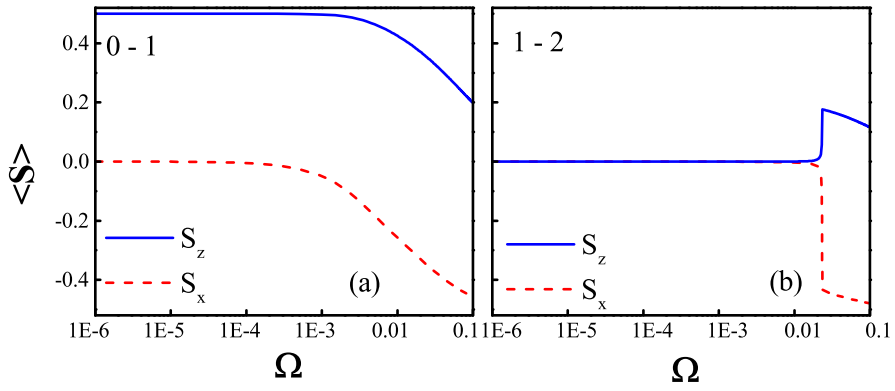

FIG. S2: The dependence of the expectation values of total spin operators in the ground state of the system on the effective tunneling Ω for the case of transition $0-1$ (a) and $1-2$ (b) for $\delta = 0.02$. Expectation value of S_y operator is always zero.

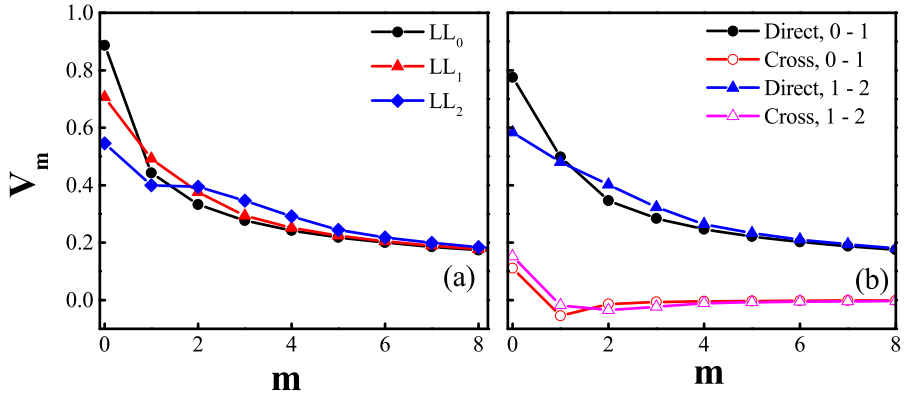

FIG. S3: Intra (a) and inter (b) LL Haldane pseudopotentials for the case of transition $0-1$ and $1-2$ as a function of relative angular momentum m.

where $V(q)$ is the Fourier transform of the Coulomb interaction. The $\mathcal{F}_{n_1,n_2}(\mathbf{q})$ is the graphene form factor defined as [3]

$$\mathcal{F}_{n_1,n_2}(\mathbf{q}) = e^{-\frac{|q|^2 l_B^2}{4}} \sqrt{\frac{(n_2-1)!}{(n_1-1)!}} \left(-\frac{\bar{q} l_B}{\sqrt{2}}\right)^{n_1-n_2} \left[C^-_{n_1} C^-_{n_2} L^{n_1-n_2}_{n_2-1}\left(\frac{|q|^2 l_B^2}{2}\right) + C^+_{n_1} C^+_{n_2} \sqrt{\frac{n_2}{n_1}} L^{n_1-n_2}_{n_2}\left(\frac{|q|^2 l_B^2}{2}\right)\right], \quad \text{(S6)}$$

when $n_1 \geq n_2$ and

$$\mathcal{F}_{n_1,n_2}(\mathbf{q}) = e^{-\frac{|q|^2 l_B^2}{4}} \sqrt{\frac{(n_1-1)!}{(n_2-1)!}} \left(\frac{q l_B}{\sqrt{2}}\right)^{n_2-n_1} \left[C^-_{n_1} C^-_{n_2} L^{n_2-n_1}_{n_1-1}\left(\frac{|q|^2 l_B^2}{2}\right) + C^+_{n_1} C^+_{n_2} \sqrt{\frac{n_1}{n_2}} L^{n_2-n_1}_{n_1}\left(\frac{|q|^2 l_B^2}{2}\right)\right], \quad \text{(S7)}$$

when $n_1 < n_2$ and we use the notation $q = q_x + iq_y$ and $\bar{q} = q_x - iq_y$ in this section.

Following the notation of table S1 the pseudopotentials which correspond to inter LL direct interaction terms are $V_m^{n_1 n_2 n_2 n_1}$, whereas the ones which correspond to inter LL cross interaction terms are $V_m^{n_1 n_2 n_1 n_2}$, where we took $n_1 \neq n_2$. As for the intra LL interaction there is just one type of pseudopotential denoted as V_m^{nnnn}. The values of appropriate pseudopotentials for both transitions $0-1$ and $1-2$ as a function of relative angular momentum m are shown in Fig. S3. The nature of intra LL pseudopotentials for graphene was analyzed before [3–5]. To understand why the physics is different for $0-1$ and $1-2$ we consider inter LL pseudopotentials shown in Fig. S3 (b). It is clear from this figure that, for relative momentum $m = 0$, the pseudopotential responsible for direct interaction terms is considerably bigger for the $0-1$ compared to the $1-2$ case, while the one responsible for cross interaction terms is slightly smaller. Due to the fact that full wave function can have even parity for the interchange of particle coordinates with different LL indices, the inter LL interaction V_0 pseudopotential makes the biggest contribution to the total inter LL interaction. The reason for the discrepancy between $0-1$ and $1-2$ stems from the two component form of the

single particle wave function of Hamiltonian of graphene shown in (1) in the main text (see also the wave function form in (2) in the main text), which for the case LL_0 has only one component non-zero. This combined with the fact that the localization for the wave function decreases with the increase of the LL index, results in having considerably larger direct type interaction for $0-1$ compared to $1-2$ case and smaller cross type of interaction. Therefore similar phases can be obtained for $0-1$ case, by either subtracting direct type or adding cross type interaction with V_0 Haldane pseudopotential. We have checked this in our calculations and obtained both the spin-singlet phase and the appropriate phase transition for $0-1$ case.

[1] G. Giuliani and G. Vignale, *Quantum Theory of the Electron Liquid* (Cambridge University Press, New York, 2005).
[2] R. E. Prange and S. M. Girvin, *The Quantum Hall Effects* (Springer-Verlag, New York, 1990).
[3] M. O. Goerbig, Rev. Mod. Phys. **83**, 1193 (2011).
[4] T. Chakraborty and V. Apalkov, in *Physics of Graphene*, edited by H. Aoki and M. S. Dresselhaus (Springer, New York, 2013) Chap. 8, pp. 251–300.
[5] Z. Papić, M. O. Goerbig, and N. Regnault, Solid State Commun. **149**, 1056 (2009).